Directed Assembly of Cylinder-Forming Block Copolymers into Patterned Structures to Fabricate Arrays of Spherical Domains and Nanoparticles

Young-Hye La, Mark P. Stoykovich, Sang-Min Park, and Paul F. Nealey*

Department of Chemical and Biological Engineering and Center for Nanotechnology, University of Wisconsin—Madison, Madison, Wisconsin 53706

Received May 4, 2007. Revised Manuscript Received June 19, 2007

The first demonstration of the directed assembly of cylindrical microdomains of a block copolymer into nonregular, patterned structures, as well as the subsequent formation of registered 1D arrays of spherical microdomains and nanoparticles, is presented. Directed assembly of pure cylinder-forming polystyrene-*block*-poly(*t*-butylacrylate) copolymer, which can undergo a cylinder-to-sphere morphological transition via thermolysis, on lithographically defined linear, circular, or angled chemical nanopatterns resulted in long-range-ordered cylindrical domains that were registered to the underlying nanopattern. Thermolysis of the cylindrical domains yields registered arrays of spherical domains, which are difficult to pattern with advanced lithographic techniques. The spherical domains maintain uniform size in all patterns studied, including 45° corners. In situ synthesis of metal and metal oxide nanoparticles within the spherical microdomains created linear, circular, and angled nanoparticle 1D arrays, registered to the chemical nanopattern. The nanoparticles within the 1D arrays were spaced uniformly, and the distance between arrays could be controlled independently of the particle size and interparticle spacing. The combined technique provides a hierarchical route for the fabrication of long-range-ordered 1D metal and metal oxide nanoparticle arrays.

Introduction

Although the interesting properties and potential applications of metal and semiconductor nanoparticles have been well documented and bulk-scale production of nanoparticles has been realized,[1,2] hurdles remain in the path to the realization of many potential applications. One such hurdle is that these applications require not only control of nanoparticle size but also control of interparticle spacing. Additionally, some applications, such as high-performance photonic/electronic circuits, telecommunication, magnetic storage media, and chemical-sensing devices, would benefit from, and in some cases require, one-dimensional (1D) nanoparticle arrays.[3] Another hurdle is, therefore, the generation of 1D nanoparticle arrays and the ability to control the spacing between arrays, which is necessary to maintain the 1D characteristics of the array. Finally, a broader range of applications would be enabled if 1D arrays could follow nonregular patterns and be registered to underlying features on the substrate. One-dimensional arrays of nanoparticles have been formed through directional assembly of nanoparticles fabricated ex situ or in situ, using templates such as organic polyelectrolytes,[4,5] biomolecules,[6−8] carbon nanotubes,[9] liquid crystalline polymers[10] and other properly structured materials.[11] Template-free assembly by magnetic-[12] or electric-dipole interactions[13] of nanoparticles and dewetting approaches[14] have also been used. However, most of these methods produced uncontrolled aggregates in addition to the locally aligned nanoparticles.

Microphase-separated morphologies of block copolymers are excellent templates as well for the in situ generation of nanoparticles in a nonconductive host matrix. Stripe-shaped nanoparticle aggregates have been successfully generated from cylindrical[15] and lamellar structures[16] of diblock copolymer thin films. Also, sphere-forming block copolymers[17] or micelles,[18] which have been functionalized chemically to enable coordination with metal ions in the cores,

* Corresponding author. E-mail: nealey@engr.wisc.edu.

(1) Alivisatos, A. P. *Science* **1996**, *271*, 933−937.
(2) Shipway, A. N.; Katz, E.; Willner, I. *Chem. Phys. Chem.* **2000**, *1*, 18−52.
(3) Tang, Z. Y.; Kotov, N. A. *Adv. Mater.* **2005**, *17*, 951−962.
(4) Kiriy, A.; Minko, S.; Gorodyska, G.; Stamm, M.; Jaeger, W. *Nano Lett.* **2002**, *2*, 881−885.
(5) Yu, S. H.; Antonietti, M.; Colfen, H.; Giersig, M. *Angew. Chem., Int. Ed.* **2002**, *41*, 2356−2360.
(6) Walsh, D.; Arcelli, L.; Ikoma, T.; Tanaka, J.; Mann, S. *Nat. Mater.* **2003**, *2*, 386−U385.
(7) Braun, E.; Eichen, Y.; Sivan, U.; Ben-Yoseph, G. *Nature* **1998**, *391*, 775−778.
(8) Warner, M. G.; Hutchison, J. E. *Nat. Mater.* **2003**, *2*, 272−277.
(9) Ajayan, P. M.; Iijima, S. *Nature* **1993**, *361*, 333−334.
(10) Mitov, M.; Portet, C.; Bourgerette, C.; Snoeck, E.; Verelst, M. *Nat. Mater.* **2002**, *1*, 229−231.
(11) Teranishi, T.; Sugawara, A.; Shimizu, T.; Miyake, M. *J. Am. Chem. Soc.* **2002**, *124*, 4210−4211.
(12) Dunin-Borkowski, R. E.; McCartney, M. R.; Posfai, M.; Frankel, R. B.; Bazylinski, D. A.; Buseck, P. R. *Eur. J. Mineral.* **2001**, *13*, 671−684.
(13) Tang, Z. Y.; Ozturk, B.; Wang, Y.; Kotov, N. A. *J. Phys. Chem. B* **2004**, *108*, 6927−6931.
(14) Huang, J. X.; Kim, F.; Tao, A. R.; Connor, S.; Yang, P. D. *Nat. Mater.* **2005**, *4*, 896−900.
(15) Lopes, W. A.; Jaeger, H. M. *Nature* **2001**, *414*, 735−738.
(16) Abes, J. I.; Cohen, R. E.; Ross, C. A. *Mater. Sci. Eng., C* **2003**, *23*, 641−650.
(17) Kane, R. S.; Cohen, R. E.; Silbey, R. *Chem. Mater.* **1996**, *8*, 1919−1924.

10.1021/cm071208n CCC: $37.00 © 2007 American Chemical Society
Published on Web 07/28/2007

have been used as nanoreactors to directly synthesize and align various metal and metal oxide nanoparticles. An advantage of the use of sphere- or micelle-forming block copolymers is that the particle size and interparticle spacing can be precisely controlled by manipulating the block copolymer domain size and periodicity. However, the final geometry generated from the scaffolds of self-organized spherical domains or micelles on the solid substrates is commonly limited to two-dimensional, close-packed hexagonal arrays.

In this research, we demonstrate a generalized approach for forming registered, nonlinear 1D arrays of metal or semiconductor nanoparticles, using as a template a block copolymer that exhibits a cylinder-to-sphere morphological transition through thermolysis. As previously described,[19] a cylinder-forming diblock copolymer, polystyrene-*block*-poly(*t*-butylacrylate) (PS-*b*-P*t*BA), on a chemically nanopatterned substrates can generate linear arrays of spherical microdomains. These registered, 1D spherical microdomains are useful for nanoscale lithographic patterning because it is inherently difficult to directly form 1D spot patterns with sphere-forming diblock copolymers. Here, we used the aligned spherical microdomains as distinct, self-limiting chemical reactors, such that chemical treatment of the film resulted in metal or semiconductor nanoparticles of precise size forming only within the spherical microdomains. The results of this combined approach were registered, nonlinear, 1D arrays of nanoparticles, in which the spacing between arrays was well-defined and controlled independently of the interparticle spacing. The technological significance of this approach is 3-fold. First, although previous research has shown that lamellae-forming copolymer/homopolymer blends can form device oriented features,[20] we demonstrate here the directed assembly of pure cylinder-forming block copolymers, registered to a nonlinear, device-oriented pattern. Second, these cylindrical domains can be converted into registered, nonlinear arrays of spherical domains, which are difficult to form directly because of the difficulties inherent in forming fine-scale spot patterns with advanced lithographical techniques. Finally, the fine control and flexibility afforded by directed assembly of block copolymers can be harnessed for nanoparticle applications, resulting in the ability to place 1D arrays of nanoparticles in desired locations and at desired spacings.

Experimental Section

Materials. Hydroxy-terminated polystyrene (HO−PS, $M_w = 9.9$ kg mol^{-1}, PDI = 1.04) was purchased from Polymer Source Inc. and used as the polymer brush for the chemically nanopatterned substrate. Photoresist-grade poly(methylmethacrylate) (PMMA, $M_w = 950$ kg mol^{-1}, 6 wt % in cholorobenzene) was purchased from Microchem Corp. Asymmetric PS-*b*-P*t*BA block copolymer ($M_w = 66.2$ kg mol^{-1} for PS and 32.0 kg mol^{-1} for P*t*BA blocks, PDI = 1.05.) was purchased from Polymer Source Inc. and provided the template for the nanoparticle 1D array formation. The bulk morphology period L_o (cylinder-to-cylinder spacing) of the PS-*b*-P*t*BA was 53 nm. Prime-grade silicon wafers (orientation ⟨100⟩) were obtained from Montoch Silicon Technologies. All materials were used as received.

Chemically Nanopatterned Substrate Formation. The silicon wafers were cleaned with piranha solution (3:7 v/v H_2O_2/H_2SO_4 at 100 °C for 30 min) before use (***Caution****: piranha reacts violently with organic compounds and should not be stored in closed containers)*. The HO−PS was spin-coated onto cleaned silicon wafers from 1.5 wt % solution in toluene at 4000 rpm. The substrates were then placed in a vacuum oven at 160 °C for 2 days to allow the therminal OH groups on the polymer chains to react with the OH groups generated in the native oxide layers of silicon wafers.[21] Ungrafted portions of the thin film were then rinsed with repeated sonication in warm toluene at least 3 times for 3 min, forming ca. 5 nm thick PS brushes. A 50 nm film of the PMMA photoresist was spin-coated on the PS brushes and patterned using extreme ultraviolet interference lithography (EUV-IL) with a transmission membrane grating for striped features ($\lambda = 13.4$ nm)[22] or electron beam lithography (20 keV, Center for Nanotechnology (CNTech), University of Wisconsin) for circular and angled features. The linear chemical patterns had periods L_s ranging from 52.5 to 60 nm in increments of 2.5 nm, and the circular and angled features had periods of 60 nm. After exposure, the photoresist was developed in a 1:3 mixture of methyl isobutyl ketone and isopropyl alcohol for 30 s, rinsed extensively with isopropyl alcohol, and blown dry in a stream of nitrogen. The topographic pattern in the photoresist was chemically transferred into the PS brush by exposing the sample to an oxygen plasma for 10 s (RF power = 100 W, O_2 flow = 8 cm^3/min). The remaining photoresist was removed by sonication in warm chlorobenzene at least 3 times for 3 min each time.

One-Dimensional Array Generation. The schematic in Figure 1 illustrates the sequence of steps in the process that we used to fabricate long-range-ordered, 1D arrays of nanoparticles from block copolymer templates directed to assemble on the chemically patterned substrates. Cylinder-forming PS-*b*-P*t*BA block copolymer was spin-coated from a 1% toluene solution onto a chemically patterned substrate to form a 45 nm thick film and then annealed at 130 °C for 2 days (step A in Figure 1**)**. After the first annealing, the samples were further heated at 150 °C for 3 days to induce the deprotection of the *t*-butyl acrylate linkages and subsequent condensation to generate poly(acrylic anhydride) ($PAA_{anhydride}$). The volume loss associated with the conversion of PS-*b*-P*t*BA to PS-*b*-$PAA_{anhydride}$ results in a morphological transformation from cylinders to spheres (step B in Figure 1). Subsequent hydrolysis in water containing a catalytic amount of acid or base at 80 °C for 1 day results in the conversion of $PAA_{anhydride}$ to poly(acrylic acid) (PAA_{COOH}).

It is well-known that the conversion of carboxylic acid functionalities to sodium carboxylate (COO^-Na^+) in the spherical domains of block copolymer thin films greatly increases both the rate and extent of metal ion uptake from metal ionic solutions through an ion-exchange reaction.[17,23,24] The PS-*b*-PAA_{COOH} thin films generated by hydrolysis were thus submerged in a 0.1 mM NaOH(aq) solution for 1 day, rinsed with DI water, and dried under a nitrogen flow to form sodium acrylate within the spherical cores.

(18) Sohn, B. H.; Choi, J. M.; Yoo, S. I.; Yun, S. H.; Zin, W. C.; Jung, J. C.; Kanehara, M.; Hirata, T.; Teranishi, T. *J. Am. Chem. Soc.* **2003**, *125*, 6368−6369.
(19) La, Y. H.; Edwards, E. W.; Park, S. M.; Nealey, P. F. *Nano Lett.* **2005**, *5*, 1379−1384.
(20) Stoykovich, M. P.; Muller, M.; Kim, S. O.; Solak, H. H.; Edwards, E. W.; de Pablo, J. J.; Nealey, P. F. *Science* **2005**, *308*, 1442−1446.
(21) Mansky, P.; Liu, Y.; Huang, E.; Russell, T. P.; Hawker, C. *Science* **1997**, *275*, 1458−1460.
(22) Solak, H. H.; David, C.; Gobrecht, J.; Golovkina, V.; Cerrina, F.; Kim, S. O.; Nealey, P. F. *Microelectron. Eng.* **2003**, *67*−*8*, 56−62.
(23) Ciebien, J. F.; Clay, R. T.; Sohn, B. H.; Cohen, R. E. *New J. Chem.* **1998**, *22*, 685−691.
(24) Clay, R. T.; Cohen, R. E. *Supramol. Sci.* **1998**, *5*, 41−48.

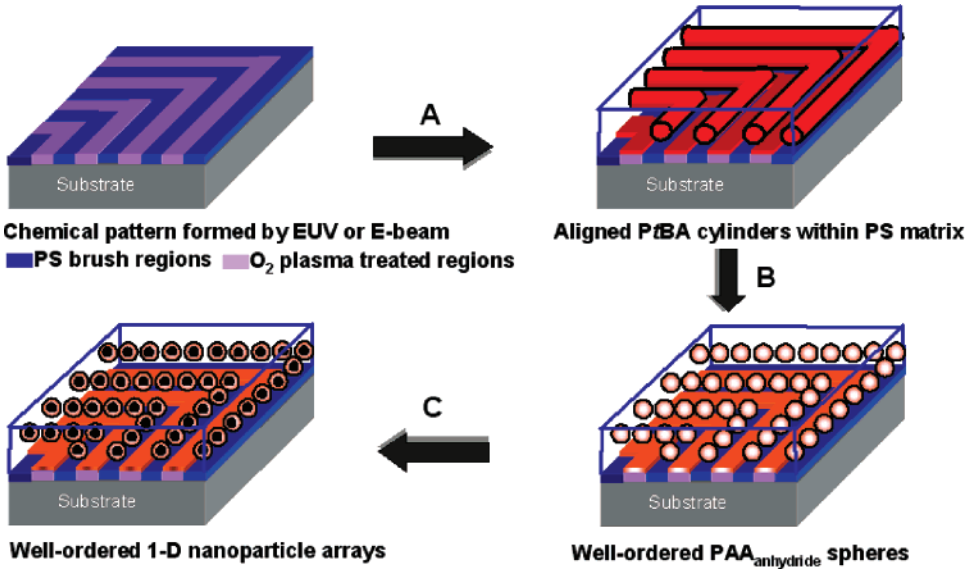

Figure 1. Schematic of the process used to fabricate long-range ordered, angled arrays of nanoparticles from block copolymer templates. (A) Spin-coated PS-*b*-PtBA on the chemically patterned substrates and annealing at 130 °C for 2 days. (B) Further annealing at 150 °C for 3 days. (C) Hydrolysis/NaOH treatment, loading metal ions, and subsequent reduction or oxidation.

Scheme 1. Chemical Transformation from [I] Poly(*t*-butyl acrylate) to Poly(acrylic anhydride) by Thermal Deprotection of the *t*-Butyl Acrylate Linkage and Subsequent Condensation, and [II] Poly(acrylic acid) Formation via Hydrolysis of Poly(acrylic anhydride)

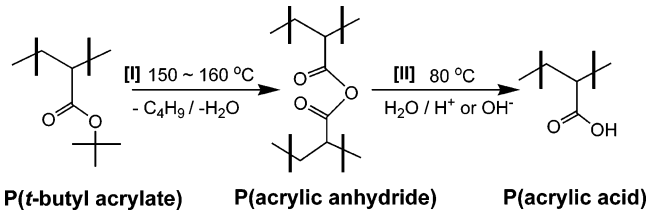

Ion exchange of the sodium with the desired metal was accomplished via exposure to the corresponding metal chloride aqueous solution. For example, for fabricating metal (Au) or metal oxide (ZnO and Fe_2O_3) nanoparticles, the films were immersed into the corresponding 1% metal chloride solutions ($AuCl_3 \cdot 6H_2O$, $ZnCl_2$, and $FeCl_3 \cdot 3H_2O$ in ethanol) for 1 h. After being rinsed with DI water and dried, the metal ions were reduced by soaking the films in a 1% $NaBH_4$(aq) solution (for Au nanoparticles) or oxidized via oxygen plasma treatment (RF power = 100 W, O_2 flow = 8 cm^3/min, for ZnO and Fe_2O_3 nanoparticles; step C in Figure 1).

Analysis. The block copolymer templates and nanoparticle arrays were imaged using a LEO 1550 VP field emission scanning electron microscopy (FE-SEM). Prior to the 1D nanoparticle arrays being arrayed, the polymer template was mostly removed with an oxygen-plasma treatment (RF power = 100 W, O_2 flow = 8 cm^3/min, 80 s). The SEM images were analyzed with a two-dimensional fast Fourier transform (FFT) algorithm to determine the average interparticle spacing, as well as the 1D array spacing. Fourier transform infrared spectroscopy (FTIR) analysis was used to study the structural changes of PS-*b*-P*t*BA diblock copolymer induced by the thermolysis and subsequent hydrolysis. The spectra were acquired with a Nicolet 860 FTIR spectrometer equipped with an MCT detector and PEM-IRRAS accessory (scan numbers = 1024, resolution = 4 cm^{-1}). X-ray photoelectron spectroscopy (XPS) measurements were performed using a Perkin-Elmer Phi 5400 instrument to confirm nanoparticle formation. Cavity formation in the hydrolyzed thin film was verified by atomic force microscopic (AFM) analysis using a Nanoscope III MultiMode AFM from Digital Instruments (tapping mode).

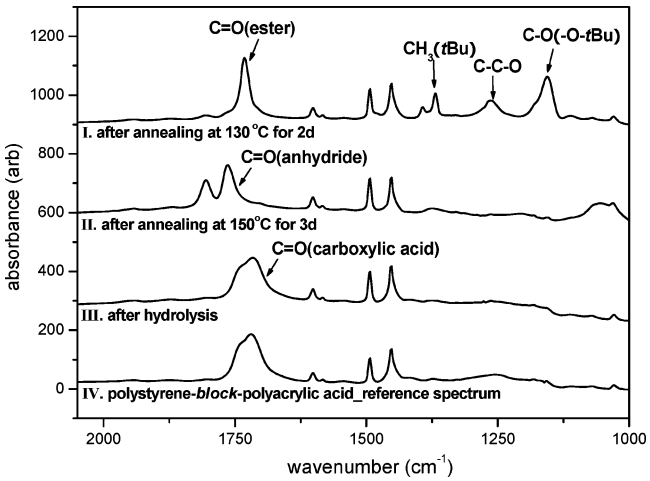

Figure 2. FTIR spectra of PS-*b*-P*t*BA diblock copolymer obtained (I) after annealing at 130 °C for 2 days, (II) after annealing at 150 °C for 3 days, and (III) after hydrolysis of sample (II). (IV) A reference spectrum of polystyrene-*block*-polyacrylic acid used to confirm the peak position of the carboxylic acid group (HO−C═O). Spectra were recorded using a Nicolet 860 FTIR spectrometer equipped with an MCT detector and PEM-IRRAS accessory (scan numbers, 1024; resolution, 4 cm^{-1}).

Results and Discussion

Linear 1D Arrays. The key to the 1D nanoparticle array formation route outlined in Figure 1 are the chemical transformations of PS-*b*-P*t*BA to PS-*b*-$PAA_{anhydride}$ to generate spherical microdomains, and then to PS-*b*-PAA_{COOH} to enable metal ion uptake (Scheme 1). The chemical transformations of the PS-*b*-P*t*BA diblock copolymer induced by the thermolysis and subsequent hydrolysis reactions were monitored by FTIR analysis on flat gold substrates, and the spectral range of interest is shown in Figure 2. The FTIR results were very similar to previous analysis of this copolymer.[19] When the copolymer film was annealed at 130 °C for 2 days, the spectrum showed absorption bands associated with *t*-butyl acrylate functionality: C═O (ester linkage) stretching, CH_3 bending, C−C−O stretching, and C−O stretching modes located at 1730, 1394/1368, 1277/

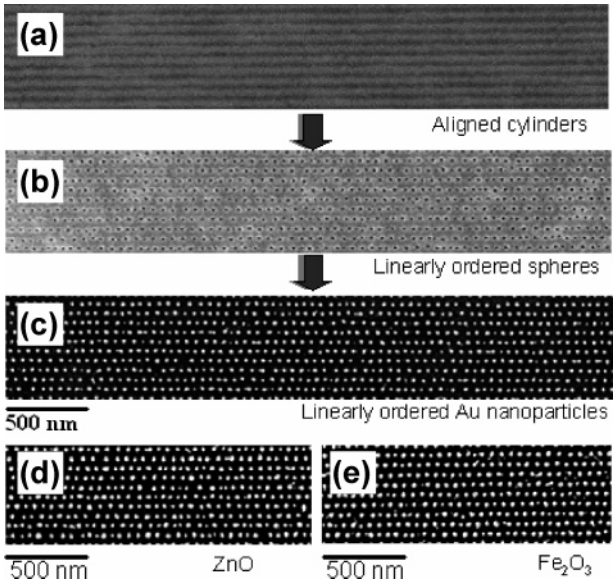

Figure 3. Plan-view SEM images of (a) self-assembled cylindrical domains of PS-*b*-P*t*BA thin film on chemically nanopatterned substrates (pattern period: 60 nm), (b) linearly ordered spherical domains of PS-*b*-$PAA_{anhydride}$ thin film that are obtained from thermolysis of sample (a), and (c) linearly ordered Au nanoparticle arrays fabricated using sample (b) as a template. (d) ZnO and (e) Fe_2O_3 nanoparticle arrays. To improve the contrast in images (a) and (b), we selectively removed the P*t*BA-related blocks with UV exposure (1.7 mW/cm^2) and acetic acid rinsing. For the nanoparticle images, the polymer templates were removed with oxygen plasma treatment.

1258, and 1160 cm^{-1}, respectively (spectrum I).[25] The characteristic peaks originating from the aromatic functionality in polystyrene also appeared between 1600 and 1400 cm^{-1}. After further annealing of this sample at 150 °C for 3 days, the peaks attributed to the *t*-butoxy group, including CH_3 bending, C−C−O stretching, and C−O stretching modes, disappeared entirely, and the sharp peak due to the carbonyl group (C═O) of the ester linkage was shifted to a higher frequency by about 30 cm^{-1} and split into two broad peaks. These peaks appeared at 1806 and 1762 cm^{-1} and represent asymmetric and symmetric stretching modes of carbonyl group in the anhydride linkages, respectively (spectrum II). The characteristic peak originating from the carboxylic acid functionality (COOH) was finally observed at 1719 cm^{-1} with a broad shape after hydrolysis of the PS-*b*-$PAA_{anhydride}$ thin film (spectrum III), and the spectrum was exactly matched with the reference spectrum we obtained from the thin film of poly(styrene)-*block*-poly(acrylic acid) (PS-*b*-PAA_{COOH}) diblock copolymer (spectrum IV).

Although the process shown in Figure 1 depicts an angled structure, the process also works for patterns consisting of parallel lines or concentric rings. The stepwise results of the process outlined in Figure 1 are displayed for a linear pattern (pattern period = 60 nm) in the SEM images shown in Figure 3. To improve the contrast in the images (images a and b in Figure 3), we selectively removed the P*t*BA-derived blocks with UV exposure and acetic acid etching.[19] The stripes in the substrate chemical nanopattern that were treated with oxygen plasma have polar hydrophilic moieties and are preferentially wetted by the P*t*BA block of the PS-*b*-P*t*BA block copolymer, whereas the stripes of unmodified PS brushes are preferentially wetted by the PS block. The preferential wetting of the chemically nanopatterned substrate directs the formation of a single layer of well-ordered P*t*BA cylinders as shown in Figure 3a.[19,26] When the PS-*b*-P*t*BA thin film aligned on the chemically nanopatterned surface was further annealed at 150 °C for 3 days, the P*t*BA cylinders were pinched off into $PAA_{anyhydride}$ spheres at regular intervals and formed well-ordered rows of spheres (Figure 3b). The average diameter of the $PAA_{anyhydride}$ spheres was ca. 22 nm, as determined by analysis of the SEM images, and the spacing between spheres in a row was ca. 51 nm, as determined by FFT analysis. After hydrolysis of the PS-*b*-$PAA_{anyhydride}$ thin film and subsequent NaOH(aq) treatment, the spherical domains were expanded to approximately 29 nm in diameter and formed COO^-Na^+ salts in the core. We also observed with AFM that the spherical domains formed cavities open to the surface in the hydrolysis. The cavity formation by swelling was similar to an earlier result reported by Cohen et al., in which the cavitated spheres provided effective metal loading as open nanoreactors.[27,28] Figure 3c shows a SEM image of the gold nanoparticle arrays obtained from the block copolymer template. Long-range-ordered 1D arrays of gold nanoparticles were successfully fabricated, and characteristic Au(4f) peaks from the gold nanoparticles were observed in X-ray photoelectron spectroscopy (XPS) spectra ($4f_{7/2}$, 84.3 eV; $4f_{5/2}$, 88.1 eV). The average diameter of the particles was 22.5 ± 1.5 nm and the average interparticle spacing (center-to-center distance within a 1-D array) was 50.6 ± 5.2 nm, which were consistent with the values observed in the block copolymer template. Metal deposition also occurred in the PAA_{COOH} wetting layers on the patterned surface, and we observed thin metal lines in the wetting layer at the substrate−film interface when we used excessive oxygen plasma treatment (see Figure S1 in the Supporting Information). We focused our analysis on the nanoparticles in the films, however, because they were formed in complete microdomains.

The fabrication strategy shown in Figure 1 can be generalized to produce various metal or metal oxide nanoparticle arrays by loading different metal ions instead of gold ion in the polymer template. Images d and e in Figure 3 show SEM images of aligned ZnO and Fe_2O_3 nanoparticle arrays prepared through selective loading of the corresponding metal ions, followed by oxidation using an oxygen plasma. During the oxygen plasma treatment, the polymer templates were simultaneously removed. The formation of nanoparticles was confirmed by XPS analysis, and characteristic Zn(2p) peaks from the ZnO particles ($2p_{1/2}$, 725.6 eV; $2p_{3/2}$, 711.4 eV) and Fe(2p) peaks from the Fe_2O_3 particles ($2p_{1/2}$, 1046.3 eV; $2p_{3/2}$, 1023.1 eV) were observed in the spectra. The diameters of the ZnO and Fe_2O_3 nanoparticles were 28.8 ± 1.2 nm and 29.0 ± 0.9 nm, respectively, which are slightly larger than the diameter of

(25) Socrates, G. *Infrared Characteristic Group Frequencies: Tables and Charts*, 2 ed.; John Wiley & Sons: New York, 1994.

(26) Edwards, E. W.; Stoykovich, M. P.; Solak, H. H.; Nealey, P. F. *Macromolecules* **2006**, *39*, 3598−3607.

(27) Boontongkong, Y.; Cohen, R. E. *Macromolecules* **2002**, *35*, 3647−3652.

(28) Bennett, R. D.; Xiong, G. Y.; Ren, Z. F.; Cohen, R. E. *Chem. Mater.* **2004**, *16*, 5589−5595.

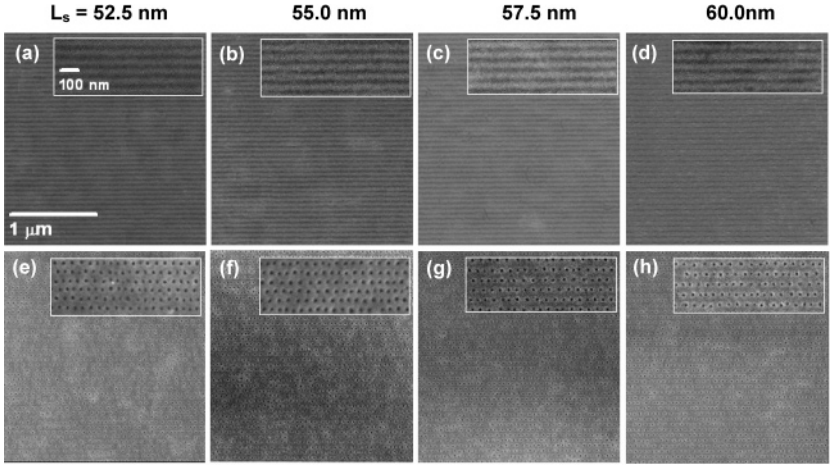

Figure 4. Plan-view SEM images of (a−d) self-assembled cylindrical domains of PS-*b*-P*t*BA thin films after annealing at 130 °C for 2 days, and (e, f) corresponding linearly aligned spherical domains of PS-*b*-$PAA_{anhydride}$ after additional annealing at 150 °C for 3 days. The spacing periods (L_s) of the underlying chemical nanopatterns for each column of image are given in the top row. To improve the contrast in the images, we selectively removed the P*t*BA blocks (dark stripes and dark spots) with UV exposure (1.7 mW/cm^2) and acetic acid rinsing.

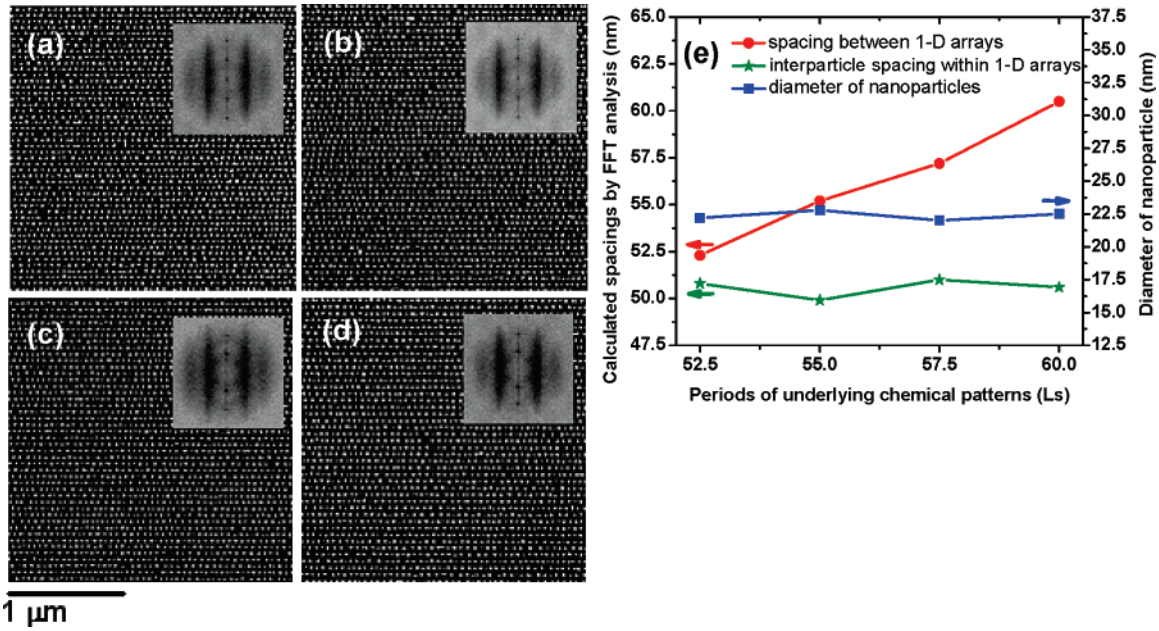

Figure 5. Plan-view SEM images of long-range ordered, linear arrays of gold nanoparticles fabricated from block copolymer templates on chemical patterns with various periods (L_s). (a) L_s = 52.5 nm, (b) L_s = 55.0 nm, (c) L_s = 57.5 nm, and (d) L_s = 60.0 nm. Inset: 2D fast Fourier transform images. (e) Plot of the calculated row-spacing (●), interparticle spacing (★), and average diameter of the particles (■) as a function of the period of underlying chemical pattern.

the Au nanoparticles. The increased nanoparticle size is likely due to oxygen incorporation that concurred with template removal during the oxidation step. The interparticle spacing, however, was consistent with the intersphere spacing of the polymer templates.

Because the cylinders or rows of spheres in the block copolymer templates conformed to the underlying chemical patterns, the spacing between rows of nanoparticles fabricated from these templates directly corresponded to the period of the original surface pattern. The row spacing is therefore tunable by applying surface patterns with different periods. Recently, we demonstrated that a high contrast in the block copolymer wetting selectivity between adjacent stripes in the chemical surface pattern induces the perfect directed assembly of cylinder-[26] and lamellar-forming[29,30] block copolymers within a certain range even though the pattern period and relative width of patterned stripes is not exactly commensurate with the domain period and width of the block copolymers. In the work presented here, the intercylinder repeat period (L_0) of the PS-*b*-P*t*BA block copolymer used as the starting material was ca. 53 nm, and near-perfect alignment of the P*t*BA cylinders was observed when the period of the underlying chemical surface pattern L_s was between 52.5 and 60 nm. The aligned P*t*BA cylinders on these chemical patterns were successfully transformed to rows of $PAA_{anhydride}$ spheres by thermolysis in a manner that conserved the original pattern periods, as shown in Figure 4a−d. The $PAA_{anhydride}$ spheres were subsequently converted

(29) Edwards, E. W.; Montague, M. F.; Solak, H. H.; Hawker, C. J.; Nealey, P. F. *Adv. Mater.* **2004**, *16*, 1315−1319.
(30) Edwards, E. W.; Muller, M.; Stoykovich, M. P.; Solak, H. H.; de Pablo, J. J.; Nealey, P. F. *Macromolecules* **2007**, *40*, 90−96.

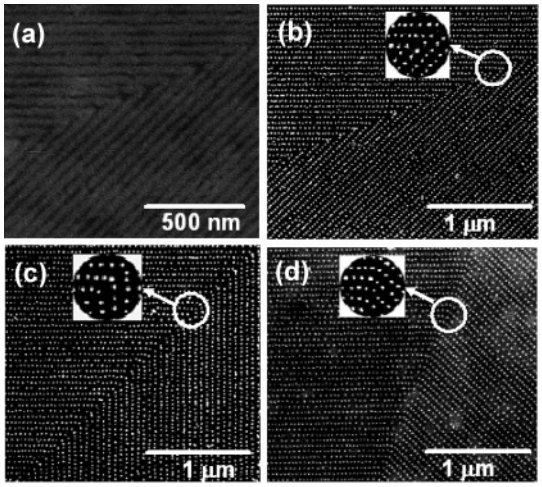

Figure 6. Plan-view SEM images of (a) P*t*BA cylinders aligned on the 45° angled chemical pattern and (b−d) gold nanopaprticle arrays fabricated from block copolymer templates in which the cylinder-to-sphere transition was induced on angle-shaped chemical patterns ((b) 45, (c) 90, and (d) 135°; pattern period, 60.0 nm). For the nanoparticle images, the polymer templates were removed with oxygen plasma treatment.

into PAA_{COOH} spheres by hydrolysis, again maintaining the original pattern geometry, spacing, and perfect registration as shown in Figure 4e−h.

The control of the spacing between the rows of the microphase-separated $PAA_{anhydride}$ spheres carried over in this work, such that we could achieve tunability of the spacing between rows of the 1D arrays of nanoparticles. Figure 5a−d shows SEM images of gold nanoparticle arrays fabricated using block copolymer templates in which the spherical domains are aligned on chemical patterns with periods of 52.5, 55.0, 57.5, and 60.0 nm. Linear arrays of gold nanoparticles were generated with long-range order in all cases. In the FFT images shown in the insets of each SEM image, the narrow, high-intensity peaks along the central vertical axis indicate that the rows of nanoparticles had regular periodicities. The broad character of the peaks parallel to the central vertical axis implies that the particles were regularly spaced within each row, but that there was no local ordering of the particles with respect to those in neighboring rows. The spacing between rows of nanoparticles and the interparticle spacing in a row were calculated by FFT analysis for these four images and plotted versus the periods of underlying chemical patterns (L_s) as shown in Figure 5e. The spacing between rows of particles exactly corresponded to the periods of the original chemical patterns (● plot), whereas the average interparticle spacing in a row (★ plot, 50.8 nm, standard deviation = 5.2 nm) was relatively constant over the entire patterned region regardless of L_s. The average diameters of the nanoparticles were estimated by image analysis and were 22.2 ± 1.2, 22.8 ± 1.4, 22.0 ± 1.2, and 22.5 ± 1.5 nm when the periods of the underlying chemical patterns were 52.5, 55.0, 57.5, and 60.0 nm, respectively. These values were also quite uniform over the extent of the patterned regions (■ plot). If necessary, the particle size and interparticle spacing can be varied by controlling the molecular weights of each block of the block copolymer template.

Nonlinear Morphologies and 1D Arrays. For practical application of nanoparticle arrays in device manufacturing, another main issue to be addressed is geometric control of the arrays. To control the nanoparticle array geometries, we must control the precursor cylindrical and spherical domain geometries. Cylinder-forming block copolymers have the ability to form various shaped structures. For example, square and circular arrangements of cylinders in PS-*b*-PMMA block copolymer thin films have been created using topographically patterned substrates.[31] The potential of cylindrical block copolymers to afford various geometries enables the creation of registered, nonregular, device-oriented arrays of spheres and, by extension, nanoparticles. Although angled, device-oriented structures have been generated previously with blends of lamellae-forming block copolymers and homopolymers on the chemical nanopatterned surfaces,[20] this was the first time that block copolymer cylinders or spheres were assembled in nonlinear, device-oriented chemical patterns. Also, in contrast to the earlier device-oriented directed assembly work, homopolymer was not added to enhance the block copolymer morphology; the device-oriented morphologies attained here were done so with 100% pure block copolymer.

To verify the versatility in geometric control, we prepared chemical patterns with characteristic features such as concentric circles or 45, 90, or 135° angles using electron beam (20 kV) lithography by following the procedure shown in

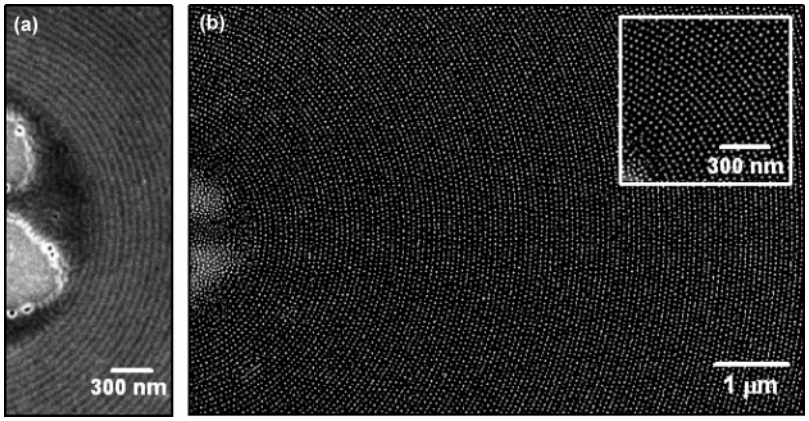

Figure 7. Plan-view SEM images of (a) P*t*BA cylinders and (b) gold nanopaprticle arrays aligned on the ringed chemical patterns (pattern period, 60.0 nm). Inset of (b): magnified image of ringed nanoparticle arrays. For the nanoparticle images, the polymer templates were removed with oxygen plasma treatment.

Figure 1, with a pattern period L_s of 60 nm. When the PS-*b*-P*t*BA block copolymer thin films were spin-coated and annealed on these nonlinear chemical patterns, the corresponding angled or ringed P*t*BA cylinders were generated without morphological defects. For example, Figure 6a shows the top-down SEM images of 45° angled P*t*BA cylinders in a PS matrix. The P*t*BA cylindrical domains perfectly self-assembled and registered in the sharp corners.

As in the case of linear 1D arrays of spherical microdomains, $PAA_{anhydride}$ spheres were then formed along the lines of original P*t*BA cylinders by further annealing of the samples at high temperature. These samples were used as templates to fabricate nanoparticle arrays after hydrolysis and subsequent NaOH treatment. Figure 6b−d shows gold nanoparticle arrays fabricated hierarchically from block copolymer templates on angle-shaped chemical patterns. The particle arrays were registered to and matched the angled chemical patterns with 45, 90, and 135° bends, even at the sharp corners. The size of nanoparticles at the sharp corners was uniform (avg. 22.3 ± 1.3 nm) and equivalent to the size of the nanoparticles on the regular lines within the error bars.

Similar results for the directed assembly of the cylinder-forming PS-*b*-P*t*BA, followed by 1D nanoparticle array formation, were obtained on a chemical pattern consisting of a set of concentric rings, as shown in Figure 7. Figure 7a shows the directed assembly of the cylindrical microdomains on the concentric rings. The center region of Figure 7a had a random morphology because it was not patterned out to a radius of 1 μm. Beyond the unpatterned core, the cylindrical domains matched the underlying chemical pattern, regardless of changes in radius of curvature. Once again, formation of spheres and then nanoparticles led to registered arrays of 1D nanoparticles, this time in concentric rings, as shown in Figure 7b. The 1D arrays conformed to the original chemical surface pattern over approximately 10 μm length scales, and the gold nanoparticles had a uniform size (21.8 ± 1.2 nm). The particle size was independent of the radius of curvature in the circular structure.

Conclusion

This work presents the first demonstration of directing the assembly of cylinder-forming block copolymers into nonlinear, device-oriented patterns. The conversion of the cylindrical domains to spherical domains led to arrays of spherical microdomains that had uniform shape even in the corners of an angled geometry. Both the cylinder domains and the arrays of spherical domains were registered to the underlying chemical pattern with long-range order.

The formation of the arrays of spherical domains registered to the underlying chemical nanopattern enabled the synthesis of registered, long-range-ordered 1D arrays of metal or metal oxide nanoparticles in a variety of geometries. Such 1D arrays are difficult to form using sphere-forming block copolymers or micelles as templates. These various geometries broaden the range of applications of 1D arrays. For example, 1D nanoparticle arrays aligned along concentric circles could find use in high-density storage media such as electric, optic, and magnetic discs.

Beyond the creation of various desired geometries of 1D arrays of nanoparticles, this technique also showed perfect registration of the arrays to the underlying patterned substrate, and good control of nanoparticle size, 1D nanoparticle arrays spacing, and interparticle spacing. The registration and the geometry of the nanoparticle arrays, as well as the spacing between rows of nanoparticles, was controlled through the underlying chemically nanopatterned substrate. Moreover, the size of the particles and the interparticle spacing should be tunable by varying the molecular weight and composition of the block copolymer templates, thereby varying the size of the initial microphase-separated polymer cylindrical domains, as well as the subsequent spherical domains in which the nanoparticles are generated.[32,33] Because of the combination of the 1D array registration capability and the independent size control of the nanoparticle spacing and the array spacing, the aligned nanoparticles can be applied to fabricating high-performance nanodevices as well as studying size- and spacing-dependent quantum mechanical properties such as electronic and photonic transfer and magnetic anisotropy in nanoparticles arrays.

Acknowledgment. This work was supported by the Semiconductor Research Corporation, the National Science Foundation, the Nanoscale Science and Engineering Center, and the Camille Dreyfus Teacher−Scholar Award. The facility and the staff of the CNTech are supported by DARPA and the Intel Corporation, and the Synchrotron Radiation Center is supported by the National Science Foundation. The authors thank Prof. B.-H. Sohn, Dr S.-H. Yun, and Dr. Gordon S. W. Craig for discussion.

Supporting Information Available: SEM image showing alternating arrays of linearly ordered nanoparticles and nanowires that were generated by complete PAA_{COOH} spheres in the film and by a PAA_{COOH} wetting layer at the substrate−film interface, respectively (PDF). This material is available free of charge via the Internet at http://pubs.acs.org.

CM071208N

(31) Black, C. T.; Bezencenet, O. *IEEE Trans. Nanotechnol.* **2004**, *3*, 412−415.

(32) Park, C.; Yoon, J.; Thomas, E. L. *Polymer* **2003**, *44*, 6725−6760.

(33) Bates, F. S.; Fredrickson, G. H. *Phys. Today* **1999**, *52*, 32−38.